Multi-meter fiber-delivery and pulse self-compression of milli-Joule femtosecond laser and fiber-aided laser-micromachining

B. Debord,[1] M. Alharbi,[1] L. Vincetti,[2] A. Husakou,[3] C. Fourcade-Dutin,[1] C. Hoenninger,[4] E. Mottay,[4] F. Gérôme,[1,5] and F. Benabid[1,5,*]

[1]*GPPMM group, Xlim Research Institute, UMR 7252 CNRS, Université de Limoges, Limoges, France*
[2]*Department of Engineering "Enzo Ferrari", University of Modena and Reggio Emilia, I-41125 Modena, Italy*
[3]*Max Born Institute, Max-Born-Str. 2a, D-12489 Berlin, Germany*
[4]*Amplitude Systèmes, 11, avenue de Canteranne, Cité de la Photonique, 33600 Pessac, France*
[5]*GLOphotonics S.A.S, Ester Technopole, 1 Avenue d'Ester, 87069 Limoges, France*
[*]*f.benabid@xlim.fr*

Abstract: We report on damage-free fiber-guidance of milli-Joule energy-level and 600-femtosecond laser pulses into hypocycloid core-contour Kagome hollow-core photonic crystal fibers. Up to 10 meter-long fibers were used to successfully deliver Yb-laser pulses in robustly single-mode fashion. Different pulse propagation regimes were demonstrated by simply changing the fiber dispersion and gas. Self-compression to ~50 fs, and intensity-level nearing petawatt/cm^2 were achieved. Finally, free focusing-optics laser-micromachining was also demonstrated on different materials.

OCIS codes: (060.5295) Photonic crystal fibers; (320.7090) Ultrafast lasers; (060.5530) Pulse propagation and temporal solitons; (350.3390) Laser materials processing.

References and links

1. M. Gu, D. Bird, D. Day, L. Fu, and D. Morrish, "Femtosecond Biophotonics, core technology and applications," Cambridge university press (2010).
2. B. N. Chichkov, C. Momma, S. Nolte, F. Alvensleben, and A. Tünnermann, "Femtosecond, picosecond and nanosecond laser ablation of solids," Appl. Phys., A Mater. Sci. Process. **63**(2), 109–115 (1996).
3. C. L. Hoy, O. Ferhanoğlu, M. Yildirim, W. Piyawattanametha, H. Ra, O. Solgaard, and A. Ben-Yakar, "Optical design and imaging performance testing of a 9.6-mm diameter femtosecond laser microsurgery probe," Opt. Express **19**(11), 10536–10552 (2011).
4. X. Liu, D. Du, and G. Mourou, "Laser Ablation and Micromachining with Ultrashort Laser Pulses," IEEE J. Quantum Electron. **33**(10), 1706–1716 (1997).
5. R. R. Gattass and E. Mazur, "Femtosecond laser micromachining in transparent materials," Nat. Photonics **2**(4), 219–225 (2008).
6. H. K. Soong and J. B. Malta, "Femtosecond lasers in ophthalmology," Am. J. Ophthalmol. **147**(2), 189–197 (2009).
7. M. H. Niemz, A. Kasenbacher, M. Strassl, A. Bäcker, A. Beyertt, D. Nickel, and A. Giesen, "Tooth ablationusing a CPA-free thin disk femtosecond laser system," Appl. Phys. B **79**(3), 269–271 (2004).
8. R. G. McCaughey, H. Sun, V. S. Rothholtz, T. Juhasz, and B. J. F. Wong, "Femtosecond laser ablation of the stapes," J. Biomed. Opt. **14**(2), 024040 (2009).
9. X. Peng, M. Mielke, and T. Booth, "High average power, high energy 1.55 μm ultra-short pulse laser beam delivery using large mode area hollow core photonic band-gap fiber," Opt. Express **19**(2), 923–932 (2011).
10. G. Humbert, J. C. Knight, G. Bouwmans, P. St. J. Russell, D. P. Williams, P. J. Roberts, and B. J. Mangan, "Hollow core photonic crystal fibers for beam delivery," Opt. Express **12**(8), 1477–1484 (2004).
11. J. A. West, C. M. Smith, N. F. Borrelli, D. C. Allan, and K. W. Koch, "Surface modes in air-core photonic band-gap fibers," Opt. Express **12**(8), 1485–1496 (2004).
12. Y. Y. Wang, X. Peng, M. Alharbi, C. F. Dutin, T. D. Bradley, F. Gérôme, M. Mielke, T. Booth, and F. Benabid, "Design and fabrication of hollow-core photonic crystal fibers for high-power ultrashort pulse transportation and pulse compression," Opt. Lett. **37**(15), 3111–3113 (2012).
13. F. Couny, F. Benabid, P. J. Roberts, P. S. Light, and M. G. Raymer, "Generation and Photonic Guidance of Multi-Octave Optical-Frequency Combs," Science **318**(5853), 1118–1121 (2007).
14. Y. Y. Wang, N. V. Wheeler, F. Couny, P. J. Roberts, and F. Benabid, "Low loss broadband transmission in hypocycloid-core Kagome hollow-core photonic crystal fiber," Opt. Lett. **36**(5), 669–671 (2011).

#208453 - $15.00 USD Received 19 Mar 2014; revised 18 Apr 2014; accepted 22 Apr 2014; published 25 Apr 2014

15. T. D. Bradley, Y. Y. Wang, M. Alharbi, B. Debord, C. Fourcade-Dutin, B. Beaudou, F. Gérôme, and F. Benabid, "Optical Properties of Low Loss (70dB/km) Hypocycloid-Core Kagome Hollow Core Photonic Crystal Fiber for Rb and Cs Based Optical Applications," J. Lightwave Technol. **31**(16), 3052–3055 (2013).
16. B. Debord, M. Alharbi, T. Bradley, C. Fourcade-Dutin, Y. Y. Wang, L. Vincetti, F. Gérôme, and F. Benabid, "Hypocycloid-shaped hollow-core photonic crystal fiber Part I: Arc curvature effect on confinement loss," Opt. Express **21**(23), 28597–28608 (2013).
17. S. Selleri, L. Vincetti, A. Cucinotta, and M. Zoboli, "Complex FEM modal solver of optical waveguides with PML boundary conditions," Opt. Quantum Electron. **33**(4/5), 359–371 (2001).
18. J. Sun and J. P. Longtin, "Inert gas beam delivery for ultrafast laser micromachining at ambient pressure," J. Appl. Phys. **89**(12), 8219 (2001).
19. F. Benabid, J. C. Knight, G. Antonopoulos, and P. St. J. Russell, "Stimulated Raman Scattering in Hydrogen-Filled Hollow-Core Photonic Crystal Fiber," Science **298**(5592), 399–402 (2002).
20. A. V. Husakou and J. Herrmann, "Supercontinuum Generation of Higher-Order Solitons by Fission in Photonic Crystal Fibers," Phys. Rev. Lett. **87**(20), 203901 (2001).
21. M. V. Ammosov, N. B. Delone, and V. B. Krainov, "Tunnel ionization of complex atoms of atomic ions in an alternating electromagnetic field," Sov. Phys. JEPT **64**, 1191–1194 (1986).
22. D. G. Ouzounov, F. R. Ahmad, D. Müller, N. Venkataraman, M. T. Gallagher, M. G. Thomas, J. Silcox, K. W. Koch, and A. L. Gaeta, "Generation of megawatt optical solitons in hollow-core photonic band-gap fibers," Science **301**(5640), 1702–1704 (2003).
23. G. Machinet, B. Debord, R. Kling, J. Lopez, F. Gérôme, F. Benabid, and P. Dupriez, "High average power and high energy transport of femtosecond pulses with a low loss Kagome hollow-core photonic crystal fiber for micromachining," CLEO Europe, CJ-11.2 THU (2013).
24. P. Jaworski, F. Yu, R. R. Maier, W. J. Wadsworth, J. C. Knight, J. D. Shephard, and D. P. Hand, "Picosecond and nanosecond pulse delivery through a hollow-core Negative Curvature Fiber for micro-machining applications," Opt. Express **21**(19), 22742–22753 (2013).

1. Introduction

The last decade witnessed a remarkable progress in ultra-short pulse (USP) lasers whereby optical pulses with durations in the sub-picosecond regime, peak-power levels higher than the Giga-Watt, and repetition rate higher than MHz are now delivered in compact tabletop and turn-key physical packages. Such an achievement contrasts with the lack of an adequate means to transport USP laser beam with no temporal or modal distortions. Today, the need for optical-waveguide to deliver USP in a robust and flexible fashion over several meter-long optical path with low attenuation is as pressing as ever as the USP technology is proving to be a transformative driver in materials micro-processing for applications as various as biophotonics [1], micro-machining [2] and micro-surgery [3]. Indeed, the unique properties of USP lasers, such its athermal material ablation characteristics, provide higher precision micro-machining in a variety of materials whilst minimizing the size of the heat affected zone [4]. These in turn are now exploited in the semiconductor industry, glass engraving, automobile and plastic electronics [5]. They are also proved to be highly useful for performing complex or delicate surgical procedures such in ophthalmic applications [6], dentistry [7] or otology [8].

A further boost to such accomplishments would be to deliver the USP laser beam in a flexible optical fiber whilst preserving the pulse power-level and temporal profile integrity during the propagation. Hitherto, the maximum USP energy level that could be guided in optical fibers is limited to nano-Joule for silica-core based optical fiber, and to a few micro-Joule for photonic bandgap (PBG) guiding hollow-core photonic crystal fiber (HC-PCF) [9]. The pulse-energy limit in solid conventional optical fiber is set by the intrinsic catastrophic material damage of the silica [4]. The limitation of PBG guiding HC-PCF is mainly due to the strong optical overlap of the core guided mode with the silica core surround [10]. This effect is exacerbated near the anti-crossing spectral range between the surface modes and the core modes [11]. In addition to the material damage limit, the fiber optical nonlinearity and dispersion are two further major limiting factors in USP waveguiding and delivery as they strongly distort the pulse temporal profile. Indeed, pulses propagating through silica will rapidly spread out due to the normal group-velocity dispersion of the material (case of wavelength below 1300 nm). As the pulse energy increases to few nano-Joule levels, there will be an additional contribution to the spreading from the Kerr and Raman responses of the

#208453 - $15.00 USD Received 19 Mar 2014; revised 18 Apr 2014; accepted 22 Apr 2014; published 25 Apr 2014

medium, which will lead to spectral broadening and yet greater dispersion. Within the above-mentioned framework, recently, up to 100 μJ energy pulses of 850 fs from a USP laser operating around 1550 nm were delivered through a 40 dB/km transmission loss hypocycloid core Kagome HC-PCF, and self-compression down to 300 fs was demonstrated [12]. These results were achieved thanks to the intrinsic properties of the guidance mechanism (coined inhibited coupling), which distinguishes from PBG guiding HC-PCF with ultra-low spatial overlap with silica and low group velocity dispersion [13]. Particularly, it was found that these performances can be further decreased by the introduction of hypocycloidal core-shaped Kagome fibers [14,15]. A systematic study on this curvature effect has recently been investigated resulting in an impressive 17 dB/km record loss value at 1 μm [16].

Here, we report on a set of experiments that demonstrate the capabilities of the hypocycloid core-shaped HC-PCF as a novel photonic platform for high-field nonlinear optics, for ultra-low loss, low temporal distortion USP guidance with unprecedented energy-level, and finally, for laser micro-machining. The paper is structured as follow. Firstly, we describe the different fibers and configurations used to demonstrate the linear properties of the USP guidance in such fibers, and which led to the record transportation of milli-Joule energy pulses of ~600 fs duration operating around 1030 nm, in a robustly single-mode fashion over up to 10 m-long hypocycloid-core Kagome HC-PCF with loss figures as low as 45 dB/km. Secondly, we investigate these fibers to demonstrate some of the nonlinear optical dynamics for the pulse propagation in fiber that are possible by simply adjusting the fiber dispersion, effective area and/or the choice of the filling gas. Here, we show that USP can be guided in a regime with a minimum temporal distortion and in a self-compression regime. For the latter regime, a self-compression down to less than 49 fs was measured, and output peak intensity nearing the petawatt/cm^2 was achieved. Finally, a flexible laser micromachining on glass, metal and semiconductor materials was demonstrated using USP laser beam that is delivered directly from the fiber output tip.

2. Fabricated HC-PCF linear properties and USP power-handling

7-cell and 19-cell hypocycloid core-shaped Kagome cladding lattice HC-PCFs were fabricated using the stack-and-draw technique. The fiber drawing parameters were set to have a fiber core contour with enhanced negative curvature [16] and to operate around the wavelength of 1030 nm. Figure 1 summarizes the physical and optical properties of the two fibers. The 19-cell hypocycloid-core Kagome HC-PCF exhibits a hypocycloid-core contour with an inner core diameter of 80 μm, corresponding to a mode field diameter (MFD) of ~64 μm. The 7-cell hypocycloid-core Kagome HC-PCF has an inner diameter of 55 μm (*i.e.* a MFD of ~44 μm). Both fibers have a silica strut thickness quite thick, 780 nm and 1300 nm respectively for the 19-cell and 7-cell designs, and a curvature parameter *b* (see definition in [16]) optimized and close to 1. The estimated numerical apertures (NA) for the 19-cell and 7-cell fibers are 0.012 and 0.018 respectively.

Figure 1 shows, for the 900-1300 nm spectral range, the spectra of the measured transmission loss (solid blue curves), the calculated waveguide group velocity dispersion (GVD) (dashed black curves), and the guided fundamental core mode optical-power overlap (PO) with the cladding silica (dot-dashed blue curves). The GVD and the PO were calculated numerically using finite-element-method with optimized perfectly matched layer [17]. Around our operating laser-wavelength of 1030 nm, the 19-cell and 7-cell fibers respectively exhibit ~200 dB/km and 45 dB/km of measured loss. The GVD was found to be + 0.8 ps/nm/km and −16 ps/nm/km for the 19-cell and 7-cell fibers respectively. Of noteworthy are the staggering PO figures of $2.8\text{x}10^{-6}$ and $4.7\text{x}10^{-5}$ for the 19-cell and 7-cell fibers respectively, which are several orders of magnitude lower than the PBG guiding HC-PCF [10]. All these characteristics make of these fibers an ideal medium to explore propagation of ultra-short duration and ultra-high power laser pulses. Moreover, the option to fill the hollow-

#208453 - $15.00 USD Received 19 Mar 2014; revised 18 Apr 2014; accepted 22 Apr 2014; published 25 Apr 2014

core by an adequate choice of the gas gives a further room of maneuver to control the fiber dispersion and nonlinear coefficient as we demonstrate it below.

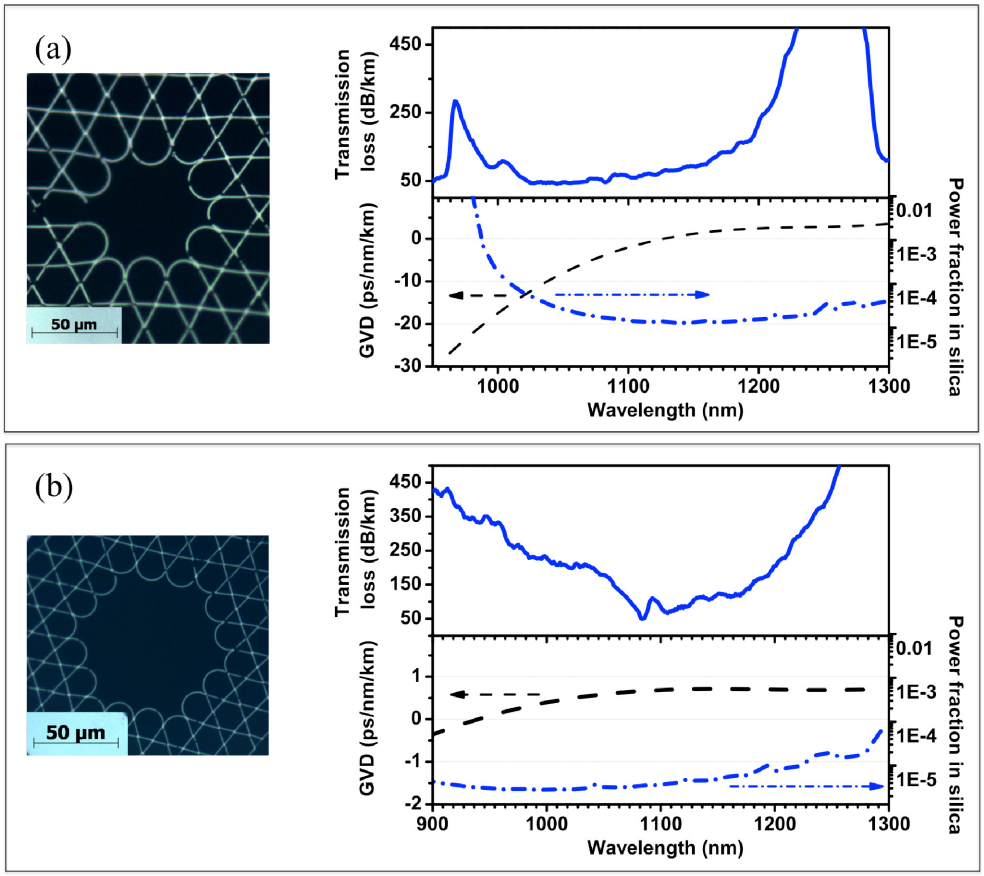

Fig. 1. Spectra of the transmission loss (blue solid curve), GVD (black dashed curve) and the PO (blue dot-dashed curve) for the 7-cell fiber (a) and 19-cell fiber (b). The optical images of the cross section of the fibers are also added.

Figure 2 summarizes the first set of experiments, and during which the linear properties of the transmission of ~600 fs pulses through the two HC-PCF types were investigated. The pulses are emitted from an Yb-based laser at repetition rate of 1 kHz and can have a maximum energy of 1 mJ. Several fiber configurations were considered to inspect the USP transmission performance and the quality of the modal content of the fiber output laser beam. The configurations comprise 3 m long and 10 m long sections from the two above-mentioned HC-PCF and were used with their core either exposed to the ambient air (air-filled configuration) or filled with helium (He-filled configuration).

The transmission results show that for He-filled 19-cell core HC-PCF a maximum of 700 µJ is transmitted when the input energy is 1 mJ (see blue solid curve in Fig. 2(a)). This level of pulse energy was achieved over several runs spaced by several hours, and with no observable damage to the fiber or degradation in the transmission coefficient. It is noteworthy that the corresponding maximum input fluence achieved here is 32 J/cm^2, which is more than one order of magnitude than the catastrophic damage threshold of the silica with sub-picosecond laser pulses [4]. To our knowledge, this is the first time that such energy level from femtosecond laser pulses can be transmitted through a single optical fiber. The

#208453 - $15.00 USD Received 19 Mar 2014; revised 18 Apr 2014; accepted 22 Apr 2014; published 25 Apr 2014

corresponding intensities will be discussed below when the pulse temporal profiles are recorded.

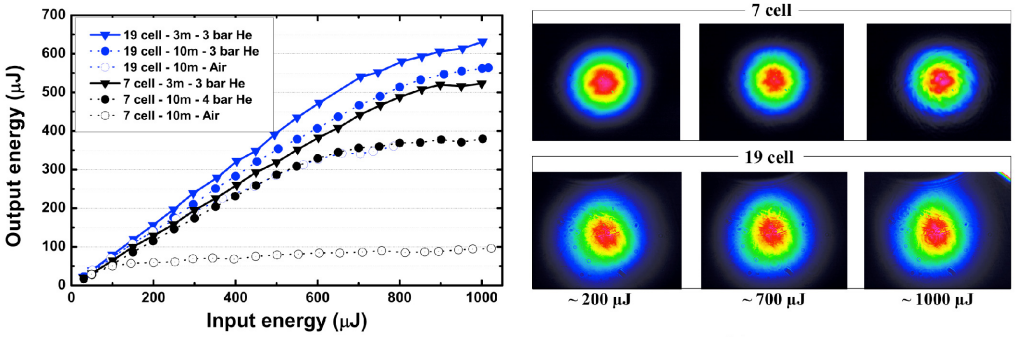

(a) (b)

Fig. 2. (a) Measured transmitted energy with input energy for 19-cell fiber (blue color-coded) and 7-cell fiber (black color-coded) for the different cases of fiber-length and gas-filling; (b) Output beam-profile evolution with input energy.

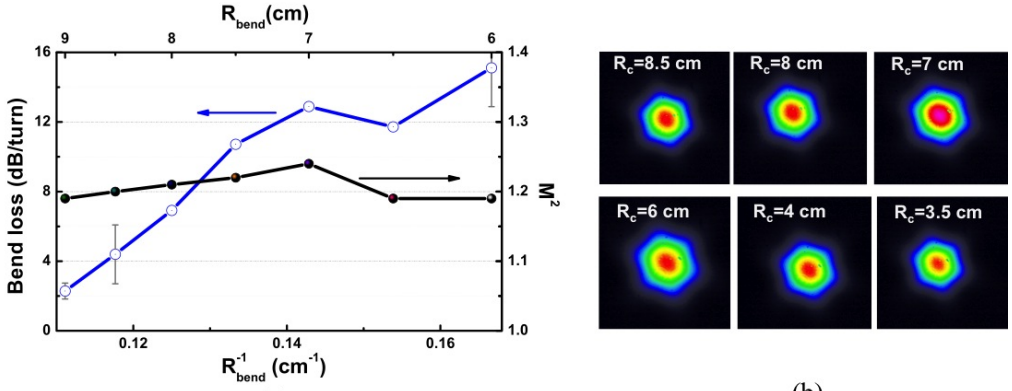

(a) (b)

Fig. 3. (a) Bend loss and M^2 evolution with bend radius and (b) near field evolution with bend radius for the 7-cell fiber design.

Furthermore, these transmission results show a strong dependence with the fiber configuration. This is illustrated by the difference in the transmission coefficient between 19-cell fiber configuration, which reaches 75%, and that of 7-cell HC-PCF configuration, which doesn't exceed 10% in the case of air-filled fiber, and 40% for He-filled for pulse-energies higher than 600 μJ. Such a drop in transmission coefficient with fiber-diameter decrease, and/or with the nature of the filling gas is resulted from the gas photoionization and the subsequent plasma absorption. Indeed, at the fiber input, the air ionization intensity threshold of 40 TW/cm^2 is reached at pulse energy of less than 300 μJ. This qualitatively agrees with the transmission curve through the 10 m long air-filled 7-cell HC-PCF (black open circle and dashed line in Fig. 2(a)), which shows a drop in the transmission slop for energies higher than 100 μJ. The pulse energy, at which the onset of such a drop in the transmission-coefficient occurs, increases when the fiber core is filled with helium and/or the fiber effective area is increased, as it is readily shown in Fig. 2(a). As a matter of fact, as it is mentioned above, with He-filled 19-cell HC-PCF, one could guide 800 μJ with no significant drop in the transmission coefficient relative to lower pulse energies. This is explained in the 5 times higher ionization threshold intensity compared to the air-filled 7-cell HC-PCF (see Table 1). Also, several measurements were done with the same fiber and no observable damage to the fiber inside-structure despite guiding pulses with fluence levels that are orders of magnitude

#208453 - $15.00 USD Received 19 Mar 2014; revised 18 Apr 2014; accepted 22 Apr 2014; published 25 Apr 2014

larger than that of the filling-gas photoionization. More remarkably, in the different fiber configurations, the light is guided in a single mode fashion for the whole laser energy-range as indicated in Fig. 2(b). The figure shows the far field output beam profiles from He-filled 7-cell and 19-cell HC-PCF for different input energies. The profiles indicate a robust single modedness for the whole input pulse energy range. This is further corroborated with Fig. 3 which summarizes the bending loss properties of these fibers. For the 7-cell design, the measured fundamental core-mode near-field (NF) and M^2~1.2 remain unchanged even for bend radius as small as 3.5 cm. For the case of the 19-cell fiber (not presented), the bending insensitivity is not as strong as the 7-cell fiber as expected due to the enlarged core size.

3. USP optical nonlinear propagation

Table 1 shows some of the relevant physical parameters for the nonlinear optical dynamics that could affect the USP guidance in the different HC-PCF configurations mentioned-above. It is readily noticeable that by simply changing the fiber configuration, one could dramatically alter these parameter ranges, and thus the propagation dynamics. For example, the dispersion length could be enhanced from 28 m for the He-filled 7-cell HC-PCF to almost 600 m for air-filled 19-cell HC-PCF. In order to demonstrate experimentally that this type of HC-PCF could indeed be an excellent and original platform to explore different high field nonlinear optical phenomena, a second set of experiments was performed.

Table 1. Dispersion length, nonlinear length, self-focusing critical power and ionization threshold intensity [18] for the different fiber configurations considered. The dispersion length is taking for gas pressure of 1 bar. The nonlinear length is calculated for the case of 1 GW peak power.

	He-filled 19 cell fiber	***Air-filled 19 cell fiber***	***He-filled 7 cell fiber***	***Air-filled 7 cell fiber***
Dispersion length, L_D (m)	555	577	28	28
Nonlinear length, L_{NL} (m)	1.9	0.09	0.9	0.04
Self-focusing critical power, P_{cr} (GW)	2026	9.5	2026	9.5
Ionization threshold intensity, I_{ii} (TW.cm^{-2})	200	40	200	40

Here, the spectral and temporal characteristics of the transmitted pulses with different energies were measured with different HC-PCF parameters. Three distinct propagation regimes have been identified and explored by simply controlling the following: the filling gas, the fiber dispersion regime and the hollow-core size (19-cell or 7-cell HC-PCF design). The first regime corresponds to high-energy USP delivery with minimum temporal and spectral distortion. Consequently, a 19-cell HC-PCF has been selected for its large core to reduce the nonlinear coefficient $\gamma = n_2\omega_0 / c\, A_{eff}$ Here, n_2, ω_0, A_{eff} and c are the fiber core nonlinear refractive index, angular frequency of the operating laser, fiber effective area and the light speed respectively. The fiber is filled with helium (3 bar at the output fiber end and 1 bar at the input end) because of its smaller nonlinear-index coefficient compared to other gas-phase media such as air, and thus to reduce further γ [12]. The gas loading is undertaken using the set-up described in [19], with the difference that one of the fiber end is left open to the ambient air. For this configuration, the nonlinear coefficient is in the range of 10^{-6} $W^{-1}km^{-1}$, which is 6 orders of magnitude lower than silica core fiber with comparable effective areas, and corresponds to nonlinear length, $L_{NL} = (\gamma P_p)^{-1}$, in excess of 1 m even for peak power P_p at GW level (see Table 1). Also, the use of the 19-cell HC-PCF allows a very small GVD and

#208453 - $15.00 USD Received 19 Mar 2014; revised 18 Apr 2014; accepted 22 Apr 2014; published 25 Apr 2014

hence very limited temporal broadening (see Fig. 1(b)). Indeed, at our operating wavelength, the GVD was calculated to be + 0.8 ps/nm/km, corresponding to $\beta_2 = -0.45 ps^2/km$, and to a dispersion length, $L_D = \tau^2/|\beta_2|$, nearing 600 m for the case of our laser input pulse duration τ of ~500 fs. Such a low nonlinear coefficient and dispersion is illustrated experimentally in Fig. 4. Figure 4(a) shows the measured output spectra of the USP laser after propagation through 3 m-long 19-cell HC-PCF and for different input pulse energies. The results show very little spectral broadening and negligible temporal distortion as it is illustrated in Fig. 4(c) (red trace). Figure 4(c) also shows the output intensity of the guided laser (black trace), which reaches a level as high as 38 TW/cm^2 when 700 μJ pulse energy (*i.e.* ~1.4 GW peak power) is coupled into the fiber.

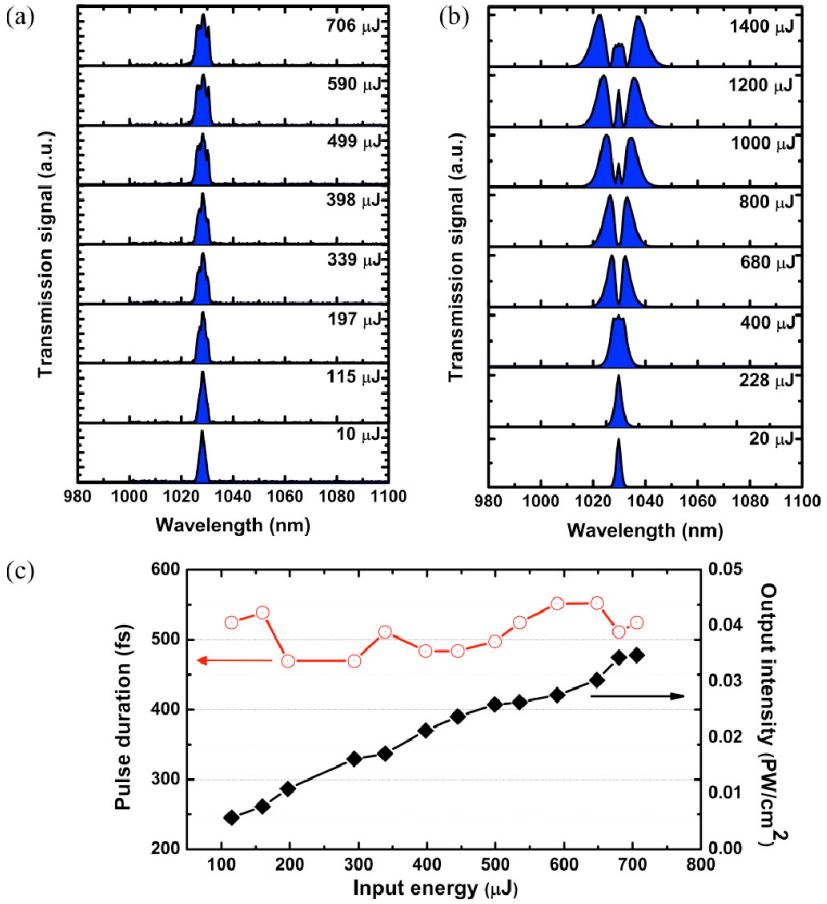

Fig. 4. High energy delivery: (a) Experimental and (b) theoretical evolution of the spectrum with input energy for the case of He-filled 19-cell HC-PCF; (c) Recorded output pulse duration and the corresponding output intensity.

The pulse propagation through the gas filled fiber was then simulated using the so-called forward Maxwell equations, which is a first-order propagation equation for the electric field, without using the slowly-varying envelope approximation [20]. In the linear part of the propagation operator, the effects of linear dispersion to all orders as well as wavelength-dependent loss were included. The data on waveguide dispersion and waveguide loss were taken from the measurement, while the dispersion of the filling gas was modelled by Sellmeyer-type formulae. The nonlinear part of the propagation accounted for the effect of the

#208453 - $15.00 USD Received 19 Mar 2014; revised 18 Apr 2014; accepted 22 Apr 2014; published 25 Apr 2014

self-phase modulation including soliton-type behavior, self-steepening, third harmonic generation, the loss of energy for the formation of plasma, as well as the time-dependent change of the refractive index due to plasma. The ADK model for the photoionization rate was utilized in the simulation [21]. Here, we have taken the ionization potentials of the main constituents of air, nitrogen and oxygen to be the same. Since the experimental research has demonstrated negligible energy transfer to the higher transverse modes of the waveguide, single-mode propagation was assumed in simulations. Figure 4(b) shows the calculation results for the 19-cell He-filled HC-PCF configuration. A good qualitative agreement with the experimental results is obtained, indicating the presence of spectra broadening due to SPM scaling linearly with the energy. Notice that the computations were running for energy higher than our experimental limit imposed by the laser performances in order to have more visibility on the dynamics.

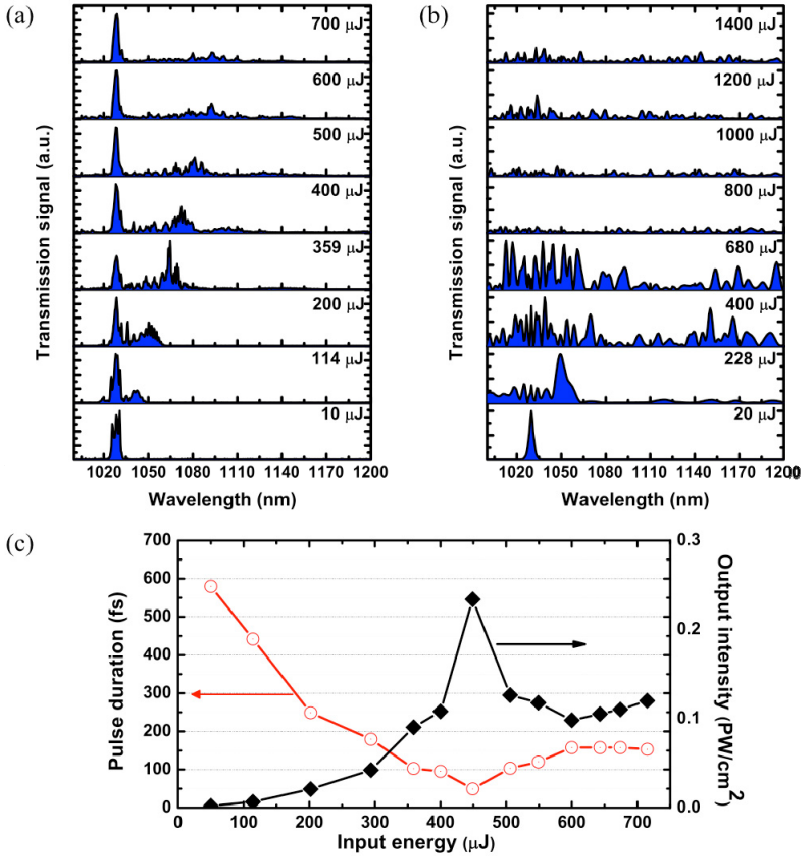

Fig. 5. Soliton self-compression: (a) Experimental and (b) theoretical evolution of the spectrum with input energy for the case of air-filled 19-cell HC-PCF; (c) Recorded output pulse duration and the corresponding output intensity.

#208453 - $15.00 USD Received 19 Mar 2014; revised 18 Apr 2014; accepted 22 Apr 2014; published 25 Apr 2014

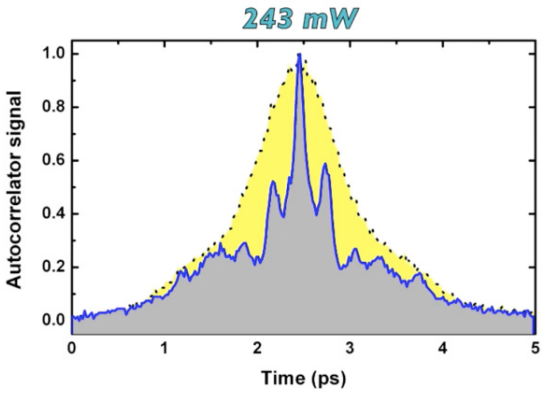

Fig. 6. Animation of the auto-correlation trace evolution with the input energy for 1.5 m long 19-cell air-filled HC-PCF (See Media 1).

Figure 5 shows the same data as in Fig. 4, but for the case of 19-cell air-filled HC-PCF. In other word, the previous 3 m-long piece of 19-cell HC-PCF is conserved with only the filling gas has changed from helium to air. According to Table 1, while the dispersion does not change significantly between the two fiber configurations, the nonlinear length, the self-focusing critical power and the ionization threshold intensity strongly differ. This change is reflected in the obtained spectra (Fig. 5(a)) and autocorrelation traces (Fig. 5(c)), which contrast with the ones of 19-cell He-filled HC-PCF. A solitonic regime is clearly observed for energy higher than 100 μJ, and which is associated with the appearance of a strong peak that red-shift relative to the pump with increasing input energy. This solitonic dynamics is further illustrated in Fig. 5(c), which shows the measured pulse duration evolution with the input pulse energy. The figure shows a strong self-compression for input pulse energies lower than 450 μJ, and minimum pulse duration of 49 fs is obtained with output energy of 280 μJ. The corresponding peak intensity reaches ~0.2 PW/cm^2 (*i.e.* peak power of ~6 GW), which is over three orders of magnitude higher than the one reported in PBG guiding HC-PCF [22]. In addition, the modeling presents a similar trend with the formation of a solitonic wave and its red-shifted spectra until to its fission into multi high-order solitons for energy scaling up to 300 μJ (Fig. 5(b)). Furthermore, Fig. 6 shows an animation of the auto-correlation trace evolution as we increased the input energy for 1.5 m long 19-cell air-filled HC-PCF. The self-compressed auto-correlation traces show the presence a very narrow peak along with a broader pedestal which is the typical signatures of a soliton and the residual the pump pulse respectively.

Finally, a third nonlinear optical regime was obtained with a 10 m-long 7-cell He-filled HC-PCF working under normal dispersion regime. Despite the very low nonlinear coefficient of Helium, a relatively strong SPM and a moderate pulse compression were observed because of the smaller effective area. Similarly to the above results, the output spectra are corroborated by the simulations (Fig. 7(b)). In this configuration, the peak intensity transmitted over the 10 m of fiber reached 90 TW/cm^2.

A full theoretical account on the pulse propagation dynamics and on the fiber properties optimization for a given aim (*i.e.* maximizing the pulse compression for example) is beyond the present paper scope and will be the subject of a future publication.

#208453 - $15.00 USD Received 19 Mar 2014; revised 18 Apr 2014; accepted 22 Apr 2014; published 25 Apr 2014

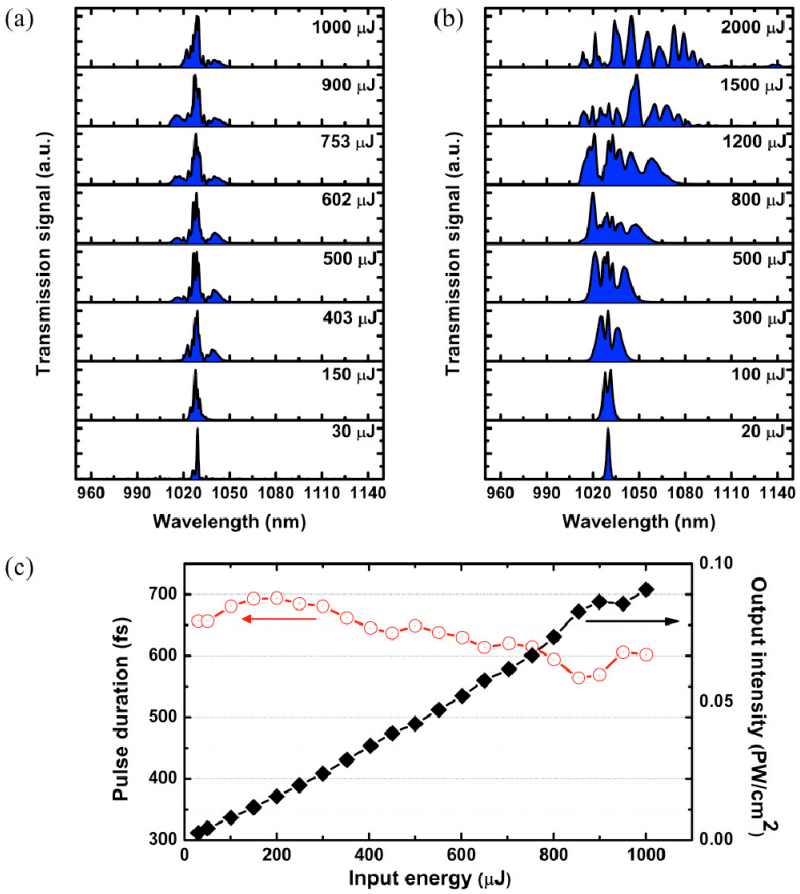

Fig. 7. SPM regime: (a) Experimental and (b) theoretical evolution of the spectrum with input energy for the case of He-filled 7-cell HC-PCF; (c) Recorded output pulse duration and the corresponding output intensity.

4. Fiber laser pen: fiber-aided micromachining

In this last section of the paper, we explore such unprecedentedly high energy level from an optical fiber delivered USP to demonstrate the concept of "fiber laser pen (FLP)" whereby laser micro-machining and micro-graving on several materials are achieved by a USP laser beam that is directly delivered from a HC-PCF output end and with no focusing lenses. The FLP was realized using a 10 m-long He-filled 19-cell HC-PCF. The fiber output pulse energy was set to below 400 μJ in order to make sure to be below the ionization regime. This configuration corresponds to a peak power intensity of ~20 TW/cm^2 representing an intensity level that is one order of magnitude higher compared to previous reports using hypocycloid-core HC-PCFs in femtosecond-regime [23] and in picosecond and nanosecond works [24].

Several samples of silicon wafer, aluminium and silica were engraved. This was achieved by placing the HC-PCF output-end on a tip of a printing tracer. Figure 8(a) shows examples of laser scribing on the different above-mentioned materials. Furthermore, in order to illustrate the cold ablation regime of micro-graving, the scribing is carried out on the tip of a match (see Fig. 8(b)). Finally, it is noteworthy that the engraving was performed directly from the fiber output tip, *i.e.* free of focusing optics, configuration possible thanks to the low numerical aperture of this fiber. Furthermore, several runs of engraving have been undertaken with the same fiber and with no recleaving to the fiber tip. This capability is illustrated in the video showing a scribing process on glass sheet (Fig. 9).

#208453 - $15.00 USD Received 19 Mar 2014; revised 18 Apr 2014; accepted 22 Apr 2014; published 25 Apr 2014

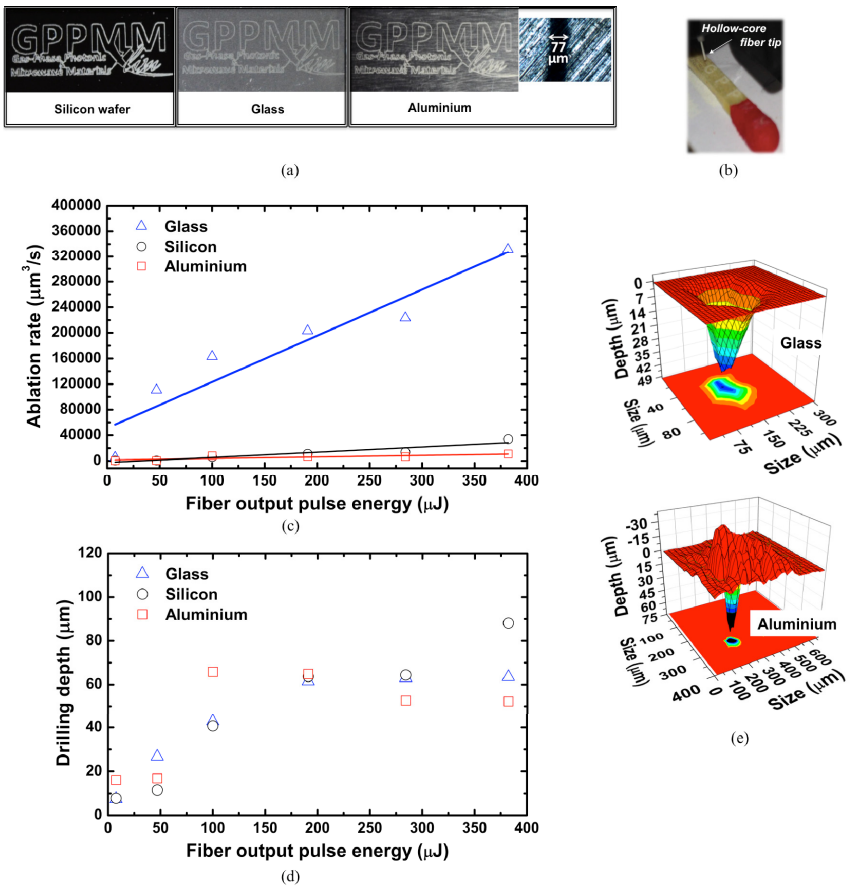

Fig. 8. (a) Laser engraving using 10 m long 19-cell HC-PCF on silicon wafer, aluminum, silica glass and (b) on highly inflammable materials; (c) The ablation rate and (d) the corresponding drilling depth evolution with the fiber delivered pulse energy; (e) A comparison of the 3D mapping of the drilling hole on glass and aluminium at 280 µJ is presented.

Fig. 9. Frame from the video showing glass sheet engraving from a USP laser beam directly delivered from the HC-PCF output end (See Media 2).

Ablation rate was then studied on the various materials for the same laser spot size and a constant 2 mm distance between the fiber tip and the material target. Figure 8(c) shows the ablation rate and Fig. 8(d) the drilling depth obtained for fiber output pulse energy range of 8 µJ-380 µJ. The minimum delivered pulse energy of 8 µJ was sufficient to perform precise graving of small patterns, less than 100 µm by 100 µm. A maximum ablation rate of 320,000

#208453 - $15.00 USD Received 19 Mar 2014; revised 18 Apr 2014; accepted 22 Apr 2014; published 25 Apr 2014

$\mu m^3/s$ for the case of the glass as plotted in Fig. 8(c). Furthermore, in the case of the glass, the ablation rate increases linearly with the pulse energy increase at a rate of 721 $\mu m^3/s$ per μJ. This contrasts with the Si wafer and aluminium where the energy increase seems to have little impact on the ablation rate. In addition, for the case of aluminium and Si wafer, the ablation rate is found to be only 20,000 $\mu m^3/s$. However, for both materials, the measurements were corrupted by a re-deposition effect of the ejected debris as shown in Fig. 8(e), and consequently, the measured of the ablation rate for Si and Aluminium is a lower-figure of the actual ablation rate if the re-deposited debris is removed during the process.

The drilling depth was also investigated and presents a maximum of 90 μm at 390 μJ on the silicon wafer (see Fig. 8(d)). The 3D mapping of the drilling hole shows a conic structure indicating a single modedness as expected. We note that this study was repeated using a 7-cell Kagome HC-PCF discussed above. Similar trends (not shown) were obtained but the results present a slight improvement of the precision of the drilling due to a smaller effective area of the fiber.

5. Conclusion

In conclusion, we experimentally demonstrated that hypocycloid core-shaped HC-PCF is an excellent platform for high field and ultra-fast optical applications. Milli-Joule level USP laser is guided over several meters long HC-PCF in either (i) a regime with minimum temporal and spectral distortion, (ii) a regime with strong soliton self-compression leading to record output peak intensity nearing the petawatt/cm^2, and more than 10-fold compression ratio in a single stage process, or (iii) in a regime where self-phase modulation dominates the nonlinear optical effect in presence. Finally, fibers as long as 10 m were used to answer industrial requirements and laser engraving was done at high energy on several materials demonstrating high-precision focus-optics free laser microprocessing.

Acknowledgments

The authors thank the PLATINOM platform for the help in the fiber fabrication and engraving 3D mapping. This research is funded by “Agence Nationale de la Recherche (ANR)” through grants PHOTOSYNTH and Σ_LIM Labex Chaire, Astrid UV-Factor and by “la région Limousin”.

#208453 - $15.00 USD Received 19 Mar 2014; revised 18 Apr 2014; accepted 22 Apr 2014; published 25 Apr 2014